Environ Earth Sci (2011) 63:533–541
DOI 10.1007/s12665-010-0715-z

ORIGINAL ARTICLE

Regional soil erosion risk mapping using RUSLE, GIS, and remote sensing: a case study in Miyun Watershed, North China

Tao Chen · Rui-qing Niu · Ping-xiang Li · Liang-pei Zhang · Bo Du

Received: 19 November 2009 / Accepted: 16 August 2010 / Published online: 31 August 2010

Abstract This paper applied the Revised Universal Soil Loss Equation (RUSLE), remote-sensing technique, and geographic information system (GIS) to map the soil erosion risk in Miyun Watershed, North China. The soil erosion parameters were evaluated in different ways: the *R* factor map was developed from the rainfall data, the *K* factor map was obtained from the soil map, the *C* factor map was generated based on a back propagation (BP) neural network method of Landsat ETM+ data with a correlation coefficient (*r*) of 0.929 to the field collected data, and a digital elevation model (DEM) with a spatial resolution of 30 m was derived from topographical map at the scale of 1:50,000 to develop the *LS* factor map. *P* factor map was assumed as 1 for the watershed because only a very small area has conservation practices. By integrating the six factor maps in GIS through pixel-based computing, the spatial distribution of soil loss in the upper watershed of Miyun reservoir was obtained by the RUSLE model. The results showed that the annual average soil loss for the upper watershed of Miyun reservoir was 9.86 t ha^{-1} ya^{-1} in 2005, and the area of 47.5 km^2 (0.3%) experiences extremely severe erosion risk, which needs suitable conservation measures to be adopted on a priority basis. The spatial distribution of erosion risk classes was 66.88% very low, 21.90% low, 6.19% moderate, 2.90% severe, and 1.84% very severe. Among all counties and cities in the study area, Huairou County is in the extremely severe level of soil erosion risk, about 39.6% of land suffer from soil erosion, while Guyuan County in the very low level of soil erosion risk suffered from 17.79% of soil erosion in 2005. Therefore, the areas which are in the extremely severe level of soil erosion risk need immediate attention from soil conservation point of view.

Keywords Risk assessment · Soil erosion · RUSLE · Remote sensing · GIS · Miyun Watershed

T. Chen (✉) · R. Niu
Institute of Geophysics and Geomatics,
China University of Geosciences, 430074 Wuhan, China
e-mail: tonychen21@gmail.com

P. Li · L. Zhang
State Key Lab of Information Engineering in Surveying,
Mapping and Remote Sensing, Wuhan University,
430079 Wuhan, China

B. Du
Computer School, Wuhan University, 430079 Wuhan, China

Introduction

The adverse influences of widespread soil erosion on soil degradation, agricultural production, water quality, hydrological systems, and environments, have long been recognized as severe problems for human sustainability (Lal 1998). And it has far-reaching economic, political, social, and environmental implications due to both on-site and off-site damages (Thampapillai and Anderson 1994; Greppe-rud 1995). Erosion and degradation not only decrease land productivity, but can also result in major downstream or off-site damage than on-site damage.

Many empirical models, based on geomorphological parameters, were developed in the past to quantify the sediment yield for assessing soil erosion from the watershed (Misra et al. 1984; Jose and Das 1982). Many other methods are extensively used for prioritization of the watersheds (Bali and Karale 1977; Wischmeier and Smith 1978). In practice, the Universal Soil Loss Equation (USLE) and later the Revised Universal Soil Loss Equation (RUSLE) have been the most widely used models in

predicting soil erosion loss. Traditionally, these models were used for local conservation planning at an individual property level. The factors used in these models were usually estimated or calculated from field measurements.

The methods of quantifying soil loss based on erosion plots possess many limitations in terms of cost, representativeness, and reliability of the resulting data. They cannot provide spatial distribution of soil erosion loss due to the constraint of limited samples in complex environments. So, mapping soil erosion in large areas is often very difficult using these traditional methods.

The use of remote sensing and geographical information system (GIS) techniques makes soil erosion estimation and its spatial distribution feasible with reasonable costs and better accuracy in larger areas (Millward and Mersey 1999; Wang et al. 2003; Boggs et al. 2001; Bartsch et al. 2002; Wilson and Lorang 2000). They showed that such methods provided significantly better results than using traditional methods. In general, remote-sensing data were primarily used to develop the cover-management factor image through land-cover classifications (Millward and Mersey 1999; Reusing et al. 2000; Ma et al. 2003), while GIS tools were used for derivation of the topographic factor from DEM data, data interpolation of sample plots, and calculation of soil erosion loss (Cerri et al. 2001; Bartsch et al. 2002; Wang et al. 2003).

The Miyun reservoir, which is situated on Chaobaihe River, supplies drinking water for Beijing, the capital of China, which has a population of 14.93 million. Sediments and nutrients from agricultural, pastoral, and forestry lands reaching the reservoir with soil erosion are the main sources of pollution, and have an impact on the safety of water supply for Beijing, and on the operation and life span of the reservoir (Zhou and Wu 2005). In terms of erosion, the soils are under a serious risk due to hilly topography, soil conditions (i.e. fine texture, low organic mater, poor plant coverage due to semi-arid climate), and inappropriate agricultural practices (excessive soil tillage and cultivation of steep lands). In order to protect the water quality, it is necessary to reduce the soil erosion in the upper stream of Miyun reservoir (Yang et al. 2005). The evaluation of current situation of erosion is very important for determining the type of conservation measures to be applied; it is very crucial to estimate the status of soil erosion, especially risk assessment, at regional-scale for sustainable management and conservation of the agricultural areas. In conclusion, the objective of this study was to use a simplified RUSLE model based on the integration of remote sensing and GIS to directly assess the soil erosion risk and to individuate areas susceptible to soil erosion requiring soil conservation planning and its application in the upper watershed of Miyun reservoir in China.

Description of the study area

The Miyun reservoir watershed is located in the northern area of Beijing (Fig. 1), between 40°19′–41°38′N and 115°25′–117°35′E with an area of about 15,788 km^2, including parts of Miyun, Huirou, and Yanqing Counties of Beijing and Guyuan, Chicheng, Chongli, Luanping, Huilai, Fengning, Xinglong, Chengde, and Zhangjiakou Counties or Cities in Hebei Province.

The northwest part of the study area is gently mountainous, while the southeast part is mainly hilly and partially plain. The altitude varies between 150 and 1,800 m above sea-level.

Climatic conditions in the area reflect the typical continental monsoon climate with 488.9 mm annual average rainfall. Distribution of precipitation is generally decreasing from southeast to northwest, and precipitations are concentrated between July and September. Annual average temperatures in upper and lower watershed are 9 and 25°C, respectively.

In this region, the soil layer is thin. According to Chinese Soil Taxonomy (Chinese Soil Taxonomy Research Group 1995), mountain meadow soil, brown forest soil, and cinnamon soil are the main soil taxa. The annual average soil erosion measured at the reservoir (Chinese River Sediment Bulletin 2006) is 12–16 t ha^{-1} and the annual amount of bedloads is about 5.72 million tons. The region suffers a severe soil erosion and it is considered a priority area for soil conservation project in China in the 21st century (Chinese River Sediment Bulletin 2006).

Satellite data image pre-processing

Four scenes of Landsat ETM+ images at spatial resolution of 30 m acquired on 14th and 21st November 2005 were used in this study (Table 1). Besides geometric correction, an atmospheric correction is required to keep images consistent. The raw image data were processed by the ENVI 4.4 software.

A digital elevation model (DEM) with a spatial resolution of 30 m was derived from topographical map at 1:50,000 scale, surveyed by State Bureau of Surveying and Mapping in 1980s.

The land use/cover maps at 1:50,000 scale in the study area were used to value the classes of the land cover (Institute of Geographic Sciences and Natural Resources Research, CAS in 1989s). The classes of land cover include farmland, forest land, grass land, water area, construction area, sandy land, meadow land, alkaline land, naked soil, and naked rock.

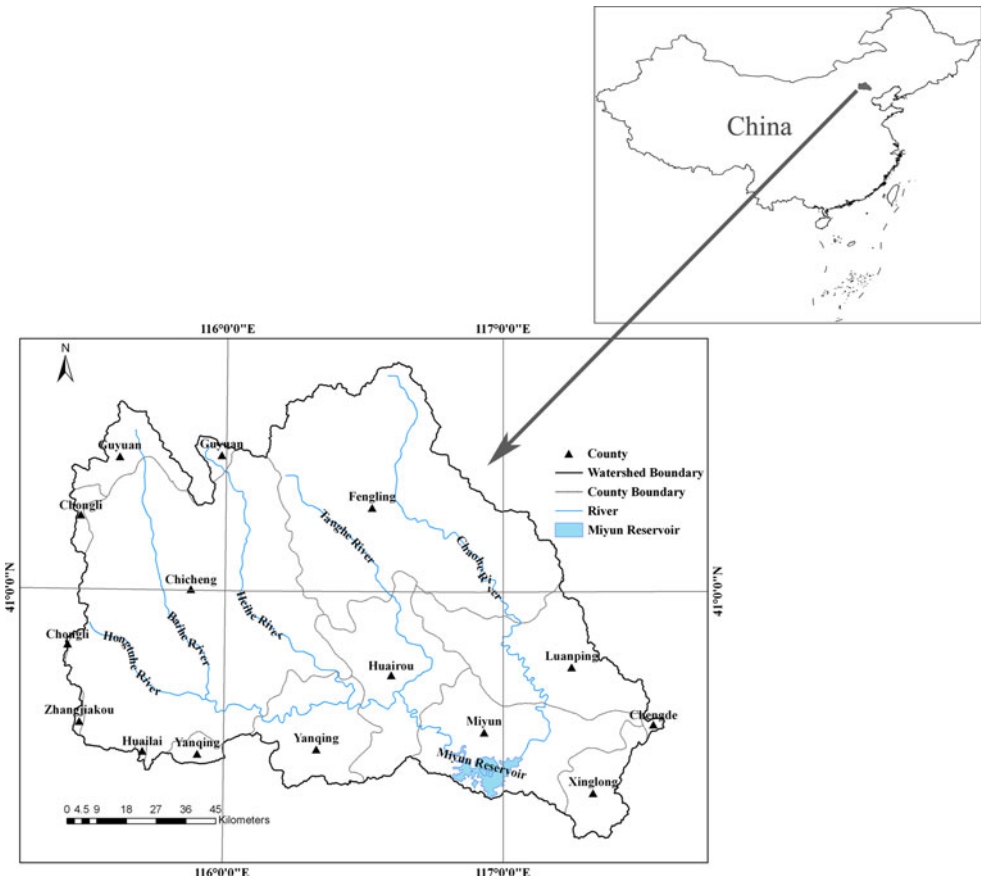

Fig. 1 Location of the study area

Table 1 Landsat ETM+ images used in the study

Image no	Path/Row	Date
1	123-031	14 Nov 2005
2	123-032	14 Nov 2005
3	124-031	21 Nov 2005
4	124-032	21 Nov 2005

Materials and methods

Classification of soil erosion in China

The study area suffers from soil erosion with higher intensity and is also at high-level risk of soil erosion. In the national professional standard of SL190-96 Standards for classification and Gradation of Soil Erosion, soil erosion intensity was divided into six degrees. With SL190-96 Standards, the monitoring of soil erosion has been successively carried out at national and regional scales in China (Zhao et al. 2002; Chen et al. 2005).

In this study, the soil erosion risk is also classified into six levels according to water and soil erosion density in SL190-96 (Table 2) (The Ministry of Water Resources of the People's Republic of China 1997; Qiao and Qiao 2002; Li and Luo 2006).

Table 2 Soil erosion risk level and intensity

Erosion risk level	Intensity	Soil loss (t ha^{-1} ya^{-1})
Very low	Slight	<10
Low	Light	10–25
Moderate	Moderate	25–50
Severe	Severe	50–80
Very severe	Very severe	80–150
Extremely severe	Extremely severe	>150

Revised Universal Soil Loss Equation

The RUSLE represents how climate, soil, topography, and land use affect rill and interrill soil erosion caused by raindrop impact and surface runoff (Renard et al. 1997). It has been extensively used to estimate soil erosion loss and to assess soil erosion risk. Moreover, the RUSLE can indicate better development and conservation plans in order to control erosion under different land-cover conditions, such as croplands, rangelands, and disturbed forest lands (Millward and Mersey 1999; Boggs et al. 2001; Mati and Veihe 2001; Angima et al. 2003). The RUSLE equation is:

$$A = R \times K \times L \times S \times C \times P \quad (1)$$

where, A is the computed amount of the average soil loss in t ha^{-1} ya^{-1}, R the rainfall erosivity factor in MJ mm ha^{-1} h^{-1} ya^{-1}, K the soil erodibility factor in t h MJ^{-1} mm^{-1}, L the slope length (m), S the slope steepness (%), C the crop management factor, and P the erosion control practice factor. Factors C and P are dimensionless.

Rainfall erosivity factor (R)

The rainfall erosivity index, R factor, in the USLE and RUSLE models, is an index of rainfall erosivity which is the potential ability of the rain to cause erosion. A storm's maximum 30-min precipitation intensity must be known to compute the storm's erosion index. If a station has not recorded 30-min intensities and only monthly and annual rainfall, the 30-min intensity of the nearest station was assumed to be representative. From long-term monthly and annual rainfall totals, and rainfall intensities from the eight meteorological stations, the rainfall R factor for each station was found by (2) (Bu et al. 2003), and the location of the rain gauges is shown in Fig. 2:

$$R_j = 0.1281 \times I_{30B} \times P_f - 0.1575 \times I_{30B} \quad (2)$$

where, P_f is annual rainfall (mm), R is mean annual erosivity (MJ mm ha^{-1} h^{-1} ya^{-1}) and I_{30B} is a storm's maximum 30-min intensity (mm/h).

Soil erodibility factor (K)

The soil erodibility factor (K), represents both susceptibility of soil to erosion and the amount and rate of runoff, as measured under standard plot conditions. The soil data used in this study were collected and derived from the Second Soil Investigation in China. For each soil type, percentages of clay, silt, and sand were used to estimate K based on the class descriptions. K was estimated using (3) (Wischmeier and Smith 1978):

$$K = [2.1 \times 10^{-4} \times (12 - a) \times [Ss \times (100 - Sc)]^{1.14} + 3.25 \times (b - 2) + 2.5 \times (c - 3)]/100 \times 0.1317 \quad (3)$$

where, K is the soil erodibility factor (t h MJ^{-1} mm^{-1}), Ss and Sc are the products of the dominant size component, and the percentage of the clay, respectively. α is the percentage of organic matter in %, b the soil structure (Table 3), c the soil saturation capability (Table 4).

Cover (C), and conservation practices (P)

In the USLE/RUSLE models, the cover factor (C) is an index which reflects, on the basis of the land use, the effect of cropping practices on the soil erosion rate. In this study, the factor C was calculated from the predominant crops using the back propagation (BP) neural network (Chen et al. 2008).

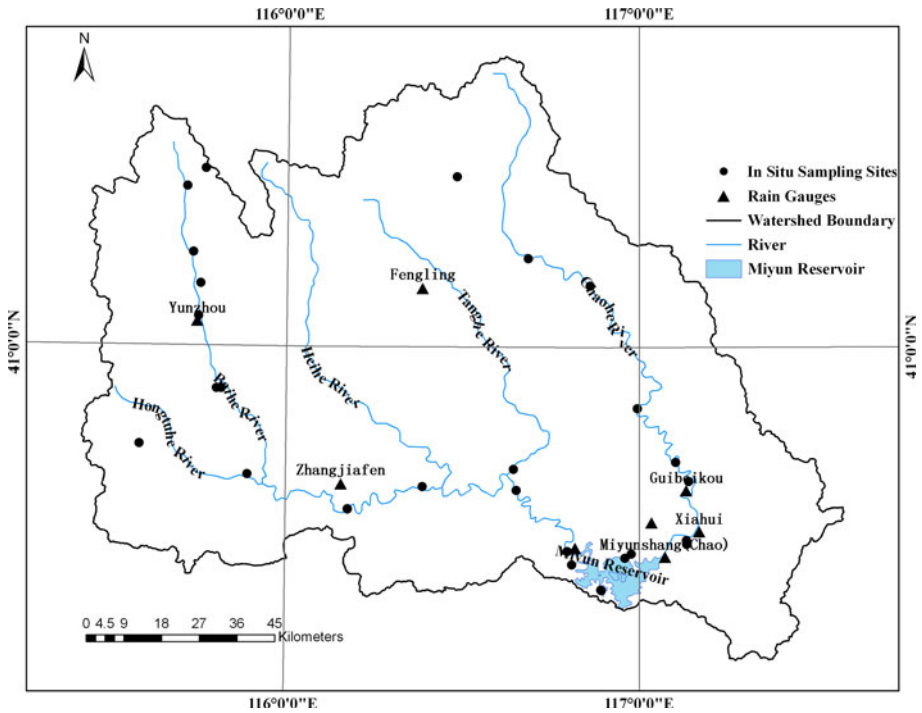

Fig. 2 Location of the rain gauges and in situ sampling sites

Table 3 Soil structure status criteria

a (%)	≤0.5	0.51–1.5	1.51–4.0	≥4.0
b	4	3	2	1

Table 4 Soil saturation capability criteria

Sc (%)	≤10	10–15.9	16–21.6	21.7–27.4	27.5–39	>39.1
c	1	2	3	4	5	6

The BP algorithm is an error-based learning process consisting of two phases. The network can be activated by the input vectors in the first phase, and the output generated through the algorithm process. The error is defined as the difference between the network output and the desired output. The error is computed in the second phase, and is then propagated backward. The total square errors are fed from the output layer back through the hidden layers to the input layer, and the connection weights can be changed accordingly. This process is repeated until the error is below a certain value, which means the propagation reaches an acceptable precision. Then the network is properly trained, and is ready for prediction.

To achieve a proper training result, several parameters need to be set up, such as the network topology structure, the number of hidden layers, the number of nodes in each hidden layer, the learning rate, the initial weight value (evenly distributed in a small range to avoid the saturation of neurons), and the training iteration times (momentum factor to avoid partial minimization). Since the method is always ambiguous, many trials are needed before the best parameter values could be determined.

Many researchers built up the relationship between vegetation index and the vegetation cover, and obtained satisfied results (Dymond et al. 1992; Graetz et al. 1988; Purevdorj et al. 1998). In this paper, three vegetation indices and their different combinations were taken as input layer to test the neural network, which were NDVI, soil adjust vegetation index (SAVI), and modified soil adjust vegetation index (MSAVI).

Finally, the network topology structure is shown in Fig. 3. The number of nodes in hidden layer is six, and the NDVI and SAVI images are taken as the input values, and the *C* factors of Miyun reservoir watershed are the output layer. As a consequence of the Stone–Weierstrass theorem, all three-layer (one hidden layer) feed-forward neural networks the neurons of which use arbitrary activation functions are capable of approaching any measurable function from one finite dimensional space to any desired degree of accuracy (Homik et al. 1989).

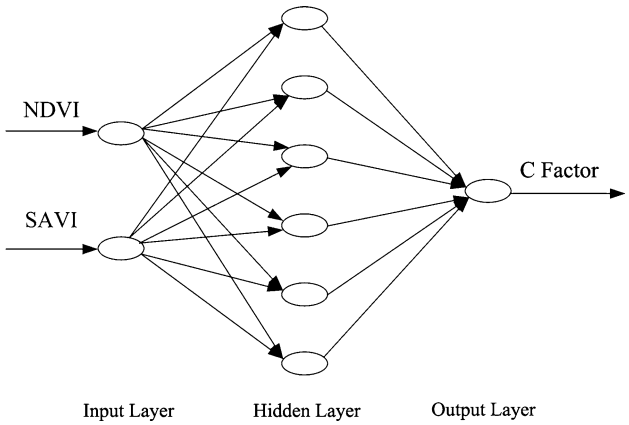

Fig. 3 Structure of the BP neural network used for *C* factor evaluation

Slope length and steepness factor (LS)

For LS calculations, the original USLE formula for estimating the slope length and slope steepness can be used (Wischmeier and Smith 1978). LS may be calculated from one of the three different functional forms of equation: linear, power, and polynomial. In this study, equation in power form is used. Liu et al. (2000) reported that an increase in the slope steepness from 20 to 40 and 60%, the slope length exponent did not change. Therefore, in the present study separate equations for slope gradient <21% as given in the USLE (4) and for areas with a slope gradient >21% as incorporated in the RUSLE (5) have been used (Renard et al. 1997; Deore 2005).

$$\mathrm{LS} = (L/22.1)^{m} \times (65.41 \times \sin^2\theta + 4.56 \times \sin\theta + 0.065) \quad (4)$$

$$\mathrm{LS} = (L/22.1)^{0.7} \times [6.432 \times \sin(\theta^{0.79}) \times \cos\theta] \quad (5)$$

where L is slope length in m, θ is angle of the slope, m is an exponent that depends on slope steepness (0.5 for slopes ≤5%, 0.4 for slopes ≤4%, and 0.3 for slopes ≤3%). m was taken as 0.5 for slopes between 5 and 21% and as 0.3 for slopes <5% in (4).

Results and discussion

By using (2), *R* values of each station were calculated. Then the input maps of *R* factor of the whole watershed were interpolated using a spline interpolation through GIS (Fig. 4). This map shows the spatial distribution of *R* values of Miyun Watershed. From Fig. 4, we can see that *R* values increased from northwest to southeast depending on precipitation characteristics. The minimum and maximum *R* value for the study area was 0.351 and 206.214 MJ mm ha^{-1} h^{-1} ya^{-1}, in 2005, respectively.

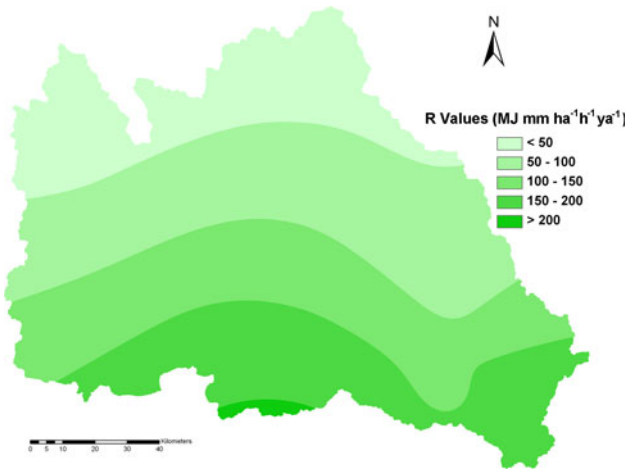

Fig. 4 *R* factor map of the study area

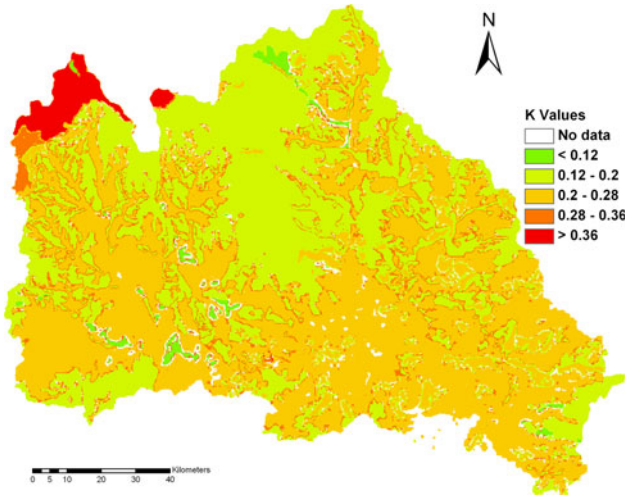

Fig. 5 *K* factor map of the study area

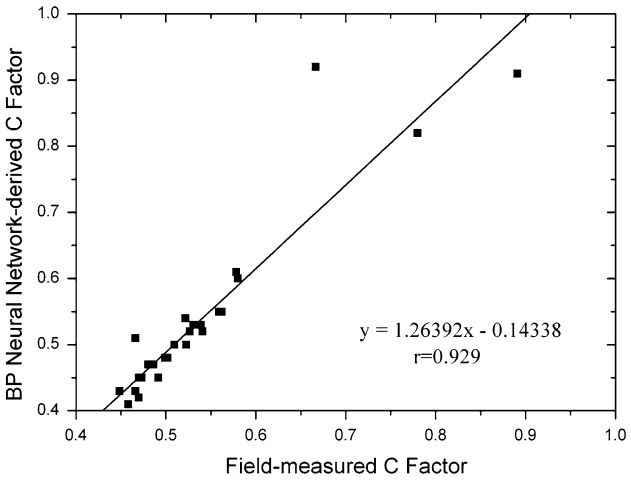

Fig. 6 Field measured *C* factor versus BP neural network-derived *C* factor

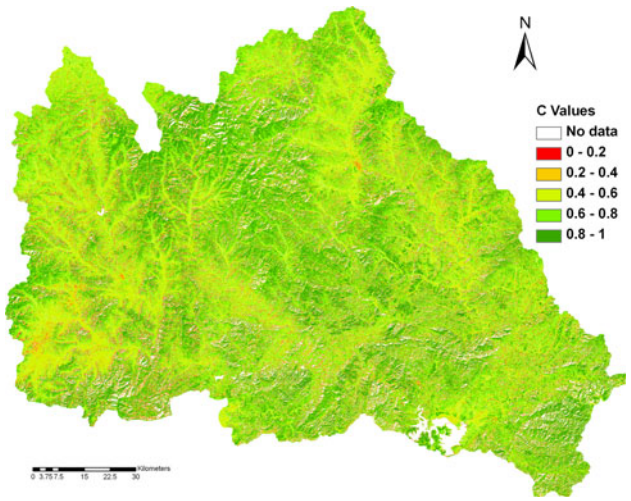

Fig. 7 *C* factor map of the study area derived using BP neural network method

R values of any place in the study area for USLE and RUSLE can be obtained from this map.

K values can be obtained by using (3). *K* values ranged from 0.117 to 0.3975 t h MJ^{-1} mm^{-1}. The map of *K* values was generated to show spatial distribution of erodibility (Fig. 5).

C values were generated from the remote-sensing data by using BP neural network method and field survey validation. Figure 6 shows the scatter plot correlations between the percentage of *C* values determined with the BP neural network and the field data from 30 sampling sites. The correlation coefficient (*r*) between the field measured *C* factor and the one which is retrieved by the BP neural network is 0.929 with the standard deviation (SD) of 0.048. The *C* factor map derived using the BP neural network is shown in Fig. 7. The *C* factor values ranged from 0.0041 to 0.1089, which were higher in the low-lying place, because they can be affected by the man-made disturbance factor. *C* factor values of any place in the study area for USLE and RUSLE can be obtained from this map. *P* factor values are assumed as 1 for the watershed, because only a very small area has conservation practices.

In this paper, a topography map with a spatial resolution of 30 m was used to develop a map of the slope length and slope steepness factor (LS) by using (4) and (5) which depends on slope smaller than 21% or more. The map obtained showed that LS values are directly related with the surface relief. LS values were higher in the mountainous area of the Miyun reservoir (Fig. 8). The highest LS value for the reservoir was calculated as 20.63.

After completing data input procedure and preparation of *R*, *K*, CP, and LS maps as data layers, they were multiplied in GIS environment to draw up the erosion risk map showing the spatial distribution of soil loss in the study

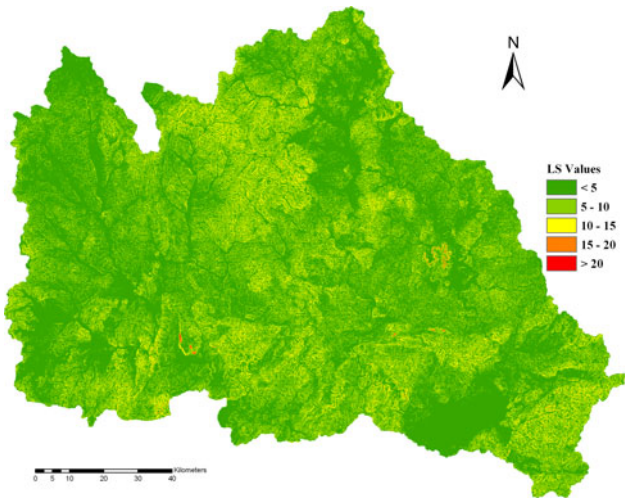

Fig. 8 LS factor map of the study area

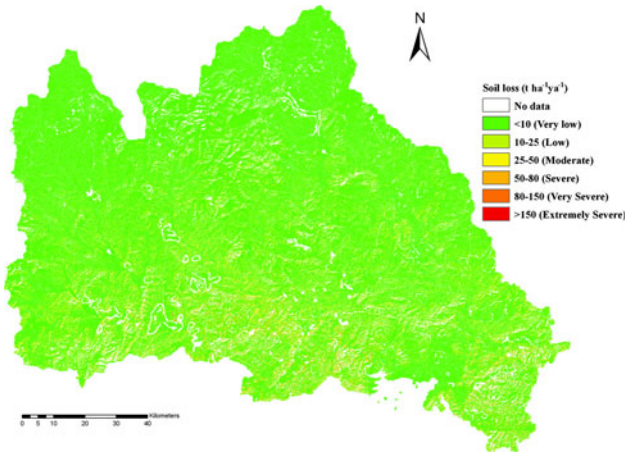

Fig. 9 Soil loss in the study area evaluated by the RUSLE method

area (Fig. 9). Average soil loss was calculated as the product of each pixel value multiplied by pixel area. Finally, the 'administration boundaries' map of the study area was overlaid on the final erosion map in order to determine erosion risk per administrative area, as shown in Table 5. Annual average soil loss for the Miyun reservoir watershed was estimated as 9.86 t ha^{-1} ya^{-1} in 2005.

In the study area, the loess hilly area has more erosion risk due to its soil erodibility. More than half of the Miyun reservoir watershed (66.88%) falls into very low erosion risk class, where soil loss is lower than 10 t ha^{-1} ya^{-1}. Soil loss increases from southeast to the northwest of the watershed. Maximum soil loss was found in the northwest part of watershed (more than 150 t ha^{-1} ya^{-1}). Huairou County is in the extremely severe level of soil erosion risk with about 39.6% of land affected by soil erosion, while Guyuan County in the very low level of soil erosion risk, with 17.79% of land affected by soil erosion.

Conclusions

The goal of this study was to assess the soil erosion risk in the Miyun Catchment (North China) for planning appropriate conservation measures. The model used to calculate average annual soil loss was the Revised Universal Soil Loss Equation (RUSLE). With a good correlation relationship of 0.929, the method offers a reliable estimate of the *C* factor on a pixel-by-pixel basis, which is useful for spatial modeling of soil erosion using the RUSLE model. Based on the BP neural network, the *C* factor values can be easily estimated by remote-sensing data with its spatial distribution.

Table 5 Soil erosion risk in the Counties of the upper watershed of Miyun reservoir in 2005

County	Total area (km^2)	Very low		Low		Moderate		Serve		Very severe		Extremely severe	
		km^2	%	km^2	%	km^2	%	km^2	%	km^2	%	km^2	%
Fengling	4,183.12	3,055.37	73.04	881.33	21.07	197.60	4.72	43.01	1.03	5.66	0.14	0.13	0.00
Chicheng	5,244.29	3,278.77	62.52	1,348.66	25.72	384.60	7.33	153.56	2.93	72.25	1.38	6.44	0.12
Chongli	111.73	91.85	82.21	18.40	16.47	1.25	1.12	0.23	0.21	0.00	0.00	0.00	0.00
Chengde	26.58	18.69	70.32	3.51	13.21	1.39	5.23	1.46	5.49	1.32	4.97	0.19	0.71
Guyuan	498.12	442.54	88.84	53.89	10.82	1.47	0.30	0.21	0.04	0.00	0.00	0.00	0.00
Huailai	16.77	11.97	71.38	2.36	14.07	1.12	6.68	0.75	4.47	0.56	3.34	0.00	0.00
Huairou	1,300.08	785.31	60.40	281.23	21.63	97.29	7.48	70.82	5.45	55.89	4.30	9.55	0.73
Luanping	1,446.14	883.34	61.08	361.35	24.99	122.15	8.45	55.43	3.83	22.76	1.57	1.10	0.08
Miyun	1,463.66	1,004.30	68.62	257.53	17.59	79.85	5.46	60.17	4.11	51.74	3.53	10.07	0.69
Xinglong	471.50	313.34	66.46	71.57	15.18	27.46	5.82	22.66	4.81	27.84	5.90	8.62	1.83
Yanqing	1,007.60	662.12	65.71	172.83	17.15	61.16	6.07	48.81	4.84	51.26	5.09	11.40	1.13
Zhangjiakou	18.45	11.61	62.93	4.36	23.63	1.28	6.94	0.71	3.85	0.49	2.66	0.00	0.00
Total	15,788.00	10,559.22	66.88	3,457.03	21.90	976.63	6.19	457.83	2.90	289.78	1.84	47.50	0.30

Results from the soil erosion risk mapping show that the soil erosion risk is higher in the northwest than in the southeast of the watershed. The regional soil erosion risk map showed that, the average soil loss found was 9.86 t ha^{-1} ya^{-1} in the watershed, and the spatial distribution of erosion risk classes was 66.88% very low, 21.90% low, 6.19% moderate, 2.90% severe, 1.84% very severe, and 0.3% extremely severe. Soils susceptible to erosion with a soil loss more than 10 t ha^{-1} ya^{-1} are found primarily in the lower watershed, especially in Huairou County. In this area, priority must be given for protection of forest and afforestation of steep bare lands and maximize plant coverage by rotation practices in the agricultural lands. Generated soil loss map is also able to indicate high erosion risk areas to soil conservationists and decision makers.

Acknowledgments This work was supported by the National Natural Science Foundation of China under Grant No. 40901205, the open fund of Key Laboratory of Agrometeorological Safeguard and Applied Technique, CMA under Grant No. AMF200905, and the open fund of State Key Lab of Information Engineering in Surveying, Mapping and Remote Sensing, Wuhan University under Grant No. 09R02.

References

Angima SD, Stott DE, O'Neill MK, Ong CK, Weesies GA (2003) Soil erosion prediction using RUSLE for central Kenyan highland conditions. Agric Ecosyst Environ 97:295–308

Bali YP, Karale RL (1977) A sediment yield index for choosing priority basins, vol 222. IAHS-AISH Publ, p 180

Bartsch KP, van Miegroet H, Boettinger J, Dobrwolski JP (2002) Using empirical erosion models and GIS to determine erosion risk at Camp Williams. J Soil Water Conserv 57:29–37

Boggs G, Devonport C, Evans K, Puig P (2001) GIS-based rapid assessment of erosion risk in a small Watershed in the wet/dry tropics of Australia. Land Degrad Dev 12(5):417–434

Bu ZH, Tang WL, Yang LZ, Xi CF, Liu FX, Wu JY, Tang HN (2003) The progress of quantitative remote sensing method for annual soil losses and its application in Taihu-Lake Watersheds. Acta Pedol Sin (in Chinese) 40(1):1–9

Cerri CEP, Dematte JAM, Ballester MVR, Martinelli LA, Victoria RL, Roose E (2001) GIS erosion risk assessment of the Piracicaba River Basin, southeastern Brazil. Mapp Sci Remote Sens 38:157–171

Chen WH, Liu LY, Zhang C, Pan YC, Wang JH, Wang JD (2005) The fast method of soil erosion investigation based on remote sensing. Res Soil Water Conserv 12:8–10

Chen T, Li PX, Zhang LP (2008) Retrieving vegetation cover by using BP neural network based on "Beijing-1" microsatellite data. In: the International conference on earth observation data processing and analysis (ICEODPA2008), 28–30 December, 2008, China

Chinese River Sediment Bulletin (2006) The Ministry of Water Resources of the People's Republic of China

Chinese Soil Taxonomy Research Group, Institute of Soil Science, Academia Sinica and Cooperative Research Group on Chinese Soil Taxonomy (1995) Chinese soil taxonomy (Revised proposal). China Agricultural Science and Technology Press, Beijing

Deore SJ (2005) Prioritization of micro-watersheds of upper Bhama Basin on the basis of soil erosion risk using remote sensing and GIS technology. Ph.D. Thesis, Department of Geography, University of Pune

Dymond JR, Stephens PR, Newsome PF, Wilde RH (1992) Percent vegetation cover of a degrading rangeland from SPOT. Int J Remote Sens 13(11):1999–2007

Graetz RD, Pech RR, Davis AW (1988) The assessment and monitoring of sparsely vegetated rangelands using calibrated Landsat data. Int J Remote Sens 9(7):1201–1222

Grepperud S (1995) Soil conservation and government policies in tropical area: does aid worsen the incentives for arresting erosion. Agric Econ 12:120–140

Homik K, Stinchcombe M, White H (1989) Multi-layer feed forward networks are universal approximators. Neural Netw 2:359–366

Jose CS, Das DC (1982) Geomorphic prediction models for sediment production rate and intensive priorities of watersheds in Mayurakshi Watershed. In: Proceedings of the international symposium on hydrological aspects of mountainous watershed held at the School of Hydrology. University of Roorkee, vol I, no 4–6, pp 15–23

Lal R (1998) Soil erosion impact on agronomic productivity and environment quality: critical reviews. Plant Sci 17:319–464

Li ZG, Luo ZD (2006) On method for evaluating soil erosion severity in county scale—index of soil erosion severity and its application. Bull Soil Water Conserv 26:41–51

Liu BY, Nearing MA, Shi PJ, Jia ZW (2000) Slope length effects on soil loss for steep slopes. Soil Sci Soc Am J 64:1759–1763

Ma JW, Xue Y, Ma CF, Wang ZG (2003) A data fusion approach for soil erosion monitoring in the Upper Yangtze River Basin of China based on Universal Soil Loss Equation (USLE) model. Int J Remote Sens 24:4777–4789

Mati BM, Veihe A (2001) Application of the USLE in a savannah environment: comparative experiences from east and west Africa. Singap J Trop Geogr 22:138–155

Millward AA, Mersey JE (1999) Adapting the RUSLE to model soil erosion potential in a mountainous tropical watershed. Catena 38:109–129

Misra N, Satyanarayana T, Mukherjee RK (1984) Effect of top elements on the sediment production rate from Sub-watershed in Upper Damodar Valley. J Agric Eng 21(3):65–70

Purevdorj TS, Tateishi R, Ishiyama T, Honda Y (1998) Relationships between percent vegetation cover and vegetation indices. Int J Remote Sens 19(18):3519–3535

Qiao YL, Qiao Y (2002) Fast soil erosion investigation and dynamic analysis in the loess plateau of China by using information composite technique. Adv Space Res 29:85–88

Renard KG, Foster GA, Weesies GA, McCool DK (1997) Predicting soil erosion by water: a guide to conservation planning with RUSLE. USDA, Agriculture Handbook No. 703, Washington, DC

Reusing M, Schneider T, Ammer U (2000) Modeling soil erosion rates in the Ethiopian Highlands by integration of high resolution MOMS-02/D2-stereo-data in a GIS. Int J Remote Sens 21:1885–1896

Thampapillai DA, Anderson JR (1994) A review of the socio-economic analysis of soil degradation problem for developed and developing countries. Rev Mark Agric Econ 62:291–315

The Ministry of Water Resources of the People's Republic of China (1997) National professional standards for classification and gradation of soil erosion, SL 190-1996

Wang G, Gertner G, Fang S, Anderson AB (2003) Mapping multiple variables for predicting soil loss by geostatistical methods with

TM images and a slope map. Photogramm Eng Remote Sens 69:889–898

Wilson JP, Lorang MS (2000) Spatial models of soil erosion and GIS. In: Fotheringham AS, Wegener M (eds) Spatial models and GIS: new potential and new models. Taylor & Francis, Philadelphia, PA, pp 83–108

Wischmeier WH, Smith DD (1978) Predicting rainfall erosion losses: a guide to conservation planning. USDA, Agriculture Handbook No. 537, Washington, DC

Yang DZ, Xu XD, Liu XD, Xu Q, Ding GA, Cheng XH, Chen HL, Zhou HG, Wang ZF, Wang WY (2005) Complex sources of air-soil-water pollution processes in the Miyun reservoir region. Sci China Ser D Earth Sci 48(Suppl II):230–245

Zhao XL, Zhang ZX, Liu B, Wang CY (2002) Method of monitoring soil erosion dynamic based on remote sensing and GIS. Bull Soil Water Conserv 22:29–32

Zhou WF, Wu BF (2005) Soil erosion estimation of the upriver areas of Miyun Reservoir located on the Chaobai River using remote sensing and GIS. Trans CSAE 21(10):46–50